J Therm Anal Calorim (2018) 131:2205–2212
https://doi.org/10.1007/s10973-017-6755-9

Thermal and morphological characterization of highly porous nanocomposites for possible application in potassium controlled release

Carlos Roberto Ferreira Junior[1] · Fabrício Nunes Tanaka[1] · Adriel Bortolin[2] · Márcia Regina de Moura[1] · Fauze Ahmad Aouada[1]

Received: 5 July 2017 / Accepted: 28 September 2017 / Published online: 11 October 2017

Abstract The use of fertilizer and water availability are essential factors limiting the agricultural production. The controlled release technology is very promising because it allows the maintenance of fertilizer concentrations within an ideal range avoiding inefficiency and toxicity problems, minimizing the environmental impacts and improving their efficiency. In this context, the nanostructured hydrogels appear as a possible carrier vehicle for these controlled release systems due to their inherent properties, such as biodegradability, low toxicity, and cost, rapid absorption and desorption controlled capacity of water and solutes. In this work, we performed the synthesis of nanostructured hydrogels based on poly(methacrylic acid) (PMAA)/Cloisite-Na^+ via free radical polymerization. SEM images indicated a similarity in the basic structure of all nanocomposites. The porous diameter of the hydrogels increased with increasing of nanoclay content. EDS analysis showed the ions belonging to nanoclay present in the nanocomposites, confirming the formation of true nanocomposites. TG–DTG and DSC techniques confirmed an improvement in the thermal stability of nanocomposites caused by the addition of nanoclay. For instance, the degradation initial temperature of the hydrogel was increased from 198.5 to 203.5 °C, and inversely, the degradation rate of the 2° thermal event was decreased from 0.694 to 0.472% min $°C^{-1}$, when the nanoclay was increased from 0 to 20 mass/%. Moreover, the controlled release investigation showed an improvement in the release time and quantity of the fertilizer released with nanoclay content. This result is very required for this specific application.

Keywords Nanocomposites · Nanoclay · Hydrogel · Morphologic properties · Thermal stability · Controlled release

Introduction

The controlled release system (CRS) was initially developed to study of drugs [1, 2]. In recent decades, the CRS is also used in formulations in agriculture. These systems are used to optimize the availability of some input in the soil. For instance, approximately 40–70% of nitrogen, 80–90% of phosphorus and 50–70% of potassium applied to the soil are lost by leaching and do not reach the plants, which not only increases costs but also leads to environmental pollution [3, 4]. In this way, CRS keeps the concentration of the substance within the minimum and maximum efficiency levels for the desired period with a single dose. The replacement of conventional formulation pesticide over CRS not only helps to avoid the remediation with excessive amounts of hazardous substances but also offers a good solution to this remediation [5, 6].

A variety of hydrogels have been employed as a carrier vehicle for agricultural CRS, such as pesticides and fertilizers, due to their intrinsic characteristics, such as low cost [7], biodegradability and non-toxicity [8, 9]. Typically, the hydrogels are three-dimensional (3D) hydrophilic

✉ Fauze Ahmad Aouada
faouada@yahoo.com.br

[1] Grupo de Compósitos e Nanocompósitos Híbridos (GCNH), Programa de Pós-Graduação em Ciência dos Materiais, School of Engineering, São Paulo State University (Unesp), Ilha Solteira, SP 15385-000, Brazil

[2] Departamento de Química, Universidade Federal de São Carlos (UFSCar), São Carlos, SP 13565-905, Brazil

polymer network chemically or physically cross-linked that have the ability to absorb a large amount of water [10, 11].

In the nanomaterial field, hybrid nanocomposites formed by polymeric matrix/inorganic nanoclay have a particular space, seeking the synergism of the individual components in the final product, which can extend its applicability [12, 13]. Natkanski et al. [13] studied the influence of hydrogel content in composite constituted by poly(acrylic acid)/montmorillonite on the Fe^{3+} adsorption capacity, as well as its thermal decomposition in various polymer/clay formulations. The authors concluded that first step of polymeric decomposition occurred around 190–367 °C, which is very similar to results described by us.

However, these matrices are very little explored. In agriculture, there is much interest in such absorbent materials containing nanoclay to control the release of herbicides and fertilizers [14]. For instance, Wilpiszewska et al. [15] prepared nanocomposites based on carboxymethyl starch (CMS) and sodium montmorillonite (MMT) cross-linked with Al^{3+} for application in controlled release of isoproturon. The authors verified that the herbicide release rate from CMS/MMT nanocomposites in water was significantly reduced when compared to commercial isoproturon, concluding that these carrier vehicles could reduce the potential leaching of such herbicide and consequently the environment pollution. In other work, Rashidzadeh and Olad [7] studied the controlled release of NPK fertilizer from sodium alginate-g-poly(acrylic acid-co-acrylamide)/montmorillonite superabsorbent nanocomposites. The authors observed a decrease in the concentration of fertilizer released from such nanocomposites, which does not occur in our study.

In other work, Bortolin et al. [5] synthesized nanocomposite hydrogels composed of polyacrylamide (PAAm), methylcellulose (MC) and calcic montmorillonite (MMT) for application in controlled release of fertilizer. The technological potential of these nanocomposites was confirmed through sorption and desorption studies of a nitrogen fertilizer, urea ($CO(NH_2)_2$). It was found that the presence of the clay mineral in the hydrogel provoked a reduction in the total amount of urea released due to strong clay–urea interactions. Inverse trend was presented in our study, i.e., greatest release of fertilizer occurred in the presence of nanoclay, what can favor its future application. The study made by Wang et al. [16] described the oscillatory swelling behavior of poly(acrylic acid) and α-zirconium phosphate ion-exchange nanoparticles. The authors proved that the water uptake process is directly related to non-equilibrium group of reactions that oscillatory swelling behavior in these specific systems is controlled by influx of Na^+ and OH^- ions. Thus, the knowledge of this behavior can provide an application in controlled drug delivery systems without external stimuli such pH and temperature variation.

The objective of this study was to investigate the influence of the nanoclay Cloisite-Na^+ on thermal properties of nanocomposites formed from poly(methacrylic acid) hydrogel and nanoclay with great applicability in agriculture. In addition, the morphological and chemical properties were investigated by SEM and EDS techniques, respectively.

Experimental

Materials

Methacrylic acid (MAA) and the initiator potassium persulfate were purchased from Aldrich. N,N′-methylenebisacrylamide (MBAAm) and monobasic potassium phosphate (KH_2PO_4) were supplied by Vetec, Brazil, and nanoclay Cloisite-Na^+ was obtained from Southern Clay Products®. All reagents were used as received.

PMAA/Cloisite-Na^+ nanocomposites synthesis

The poly(methacrylic acid)/Cloisite-Na^+ (PMAA/Clay) nanocomposite hydrogels cross-linked by N,N′-methylenebisacrylamide—MBAAm (C_{final} = 2% molar in relation to MAA monomer), were synthesized via free radical polymerization started by potassium persulfate (C_{final} = 3.1 mmol L^{-1}) as described by Junior et al. [17]. MAA concentration was fixed at 7.5% (m v^{-1}), and nanoclay concentration was varied from 0 to 20 mass/%.

Scanning electron microscopy (SEM) and energy-dispersive X-ray spectroscopy (EDS)

The hydrogels, swollen in distilled water at room temperature until equilibrium stage, were quickly frozen in liquid nitrogen and freeze-dried at − 55 °C for 24 h in a lyophilizer model Enterprise II Terroni. Then, the freeze-dried hydrogels were coated with a thin gold layer, and the morphology and chemical microanalysis were observed by ZEISS EVO LS15 electronic microscope operating at 20 kV.

Thermogravimetric analysis (TG)

Approximately 8–10 mg was heated from room temperature to 800 °C, at 10 °C min^{-1}, with nitrogen gas flows of 40 and 60 mL min^{-1} in the balance and sample, respectively. A TA Instruments model TGA Q-500 was used in the experiments.

Differential scanning calorimetry (DSC)

The DSC analysis was carried out using a TA Instruments model DSC Q100. Approximately 3–5 mg of each dry sample was accurately weighed into closed aluminum pan and then heated at 10 °C min^{-1} from − 50 to 250 °C using nitrogen flow of 60 mL min^{-1}.

Controlled release studies

In these studies, the potential of nanocomposite hydrogels in relation to release of monobasic potassium phosphate (KH_2PO_4) was evaluated. For this, the hydrogels with 0 and 20% nanoclay were swollen in 100 mL of KH_2PO_4 aqueous solution at 2000 ppm until equilibrium state (around 7 days). After this procedure, the hydrogels were transferred to a beaker containing 100 mL of distilled water, and the conductivity measurements were quantified by a digital CG 2000 GEHAKA conductivimeter, using a calibration curve.

Results and discussion

Scanning electron microscopy (SEM) and energy-dispersive X-ray spectroscopy (EDS)

SEM technique was employed to investigate the surface of nanoclay Cloisite-Na^+ and internal morphologies of hydrogels and their nanocomposites, as shown in Fig. 1a. It was possible to see that the nanoclay had compacted and aggregate aspect and that regions were bulky with different sizes and formats [18]. In Fig. 1b, it was possible to observe that the PMAA/0-nanoclay hydrogel had a honeycomb-like porous structure homogeneously distributed on the whole surface. Pores with these characteristics provide the means of transport of water to interior or exterior of the matrix [19].

Nanocomposites composed by PMAA/10 and 20-nanoclay presented similar structure, i.e., morphology highly porous with well-homogeneous distribution. The average porous size, calculated from an adaptation of ASTM E-112 norm, was dependent of nanoclay content in the solution-forming hydrogel. Pure hydrogel (or hydrogel without nanoclay) and PMAA/10 nanocomposite exhibited a pore average diameter values of 13.9 ± 0.3 and 14.4 ± 0.1 μm, respectively. Already, the nanocomposite prepared with highest nanoclay content presented the highest pore size, approximately 15.0 ± 0.3 μm. This trend confirmed the high-water absorption capacity of these nanocomposites previously described by our research group [17]. Moreover, Fig. 2b, c shows a slight roughness, mainly in nanocomposites with 20% Cloisite-Na^+, differently of pure hydrogel (Fig. 2a), and still, nanoclay agglomeration points are highlighted by the red circle in Fig. 2d.

Analysis of EDS (Fig. 1a'–d') shows that the elements belonging to nanoclay (Na, Mg, Al and Si) are present in the synthesized nanocomposites, confirming that, even after purification and freeze-drying process, the nanoclay is maintained in the nanocomposite structure, characterizing the formation of true nanocomposites.

Thermogravimetric analysis (TG)

According to the TG curve (Fig. 3), the thermal decomposition of the Cloisite-Na^+ occurs in two main events: the first one occurred before 100 °C that is associated with the loss of water of hydration; the second one between 550 and 700 °C, resulting from the dehydroxylation of the layers of nanoclay [20, 21]. For the PMAA/n-nanoclay systems, four main events were identified. An initial mass loss below 100 °C is also related to the release of water or other volatiles. The second event at 200–297 °C corresponds to the decarboxylation of the PMAA polymer, leading to the formation of six-member cyclic anhydride [22, 23]. The third event at 302–450 °C is associated with the imidization of MBAAm chains and release of ammonia (NH_3), and the fourth event at 450–570 °C is resulting in the complete degradation of the polymer (or pyrolysis) [24, 25].

The increase in nanoclay provoked an increase in the initial temperature (T_i) of the second event, indicating an improvement in the thermal stability of the nanocomposites (Table 1). Likely, the nanolayers act as barriers by increasing the thermal isolation (Scheme 1), minimizing the permeability of products of degradation in the material [26]. The decrease in the degradation rate (% min $°C^{-1}$) of the 2° event with increasing of nanoclay concentration in the matrix also proved the increase in the thermal stability. An increase in the residue (from 2% or 0.20 mg for the pure hydrogel to 13% or 1.08 mg for hydrogel with 20% nanoclay) after the end of thermal decomposition (Fig. 4) was also observed. This behavior was expected, whereas the nanoclay is very thermally stable presenting little mass loss in the investigated temperature. Similar trends using poly(acrylic acid)/montmorillonite hydrogels were observed by Natkanski et al. [13].

Differential scanning calorimetry (DSC)

In all DSC curves was identified a first endothermic peak around 100 °C attributed to the loss of bound water and possible volatiles associated with the hydrophilic groups of the polymer chain [27, 28], as shown in Fig. 5. The area of this peak, corresponding to the variation of enthalpy (ΔH) necessary to occur the phase transformation of the water (liquid to vapor state), decreased with the addition of

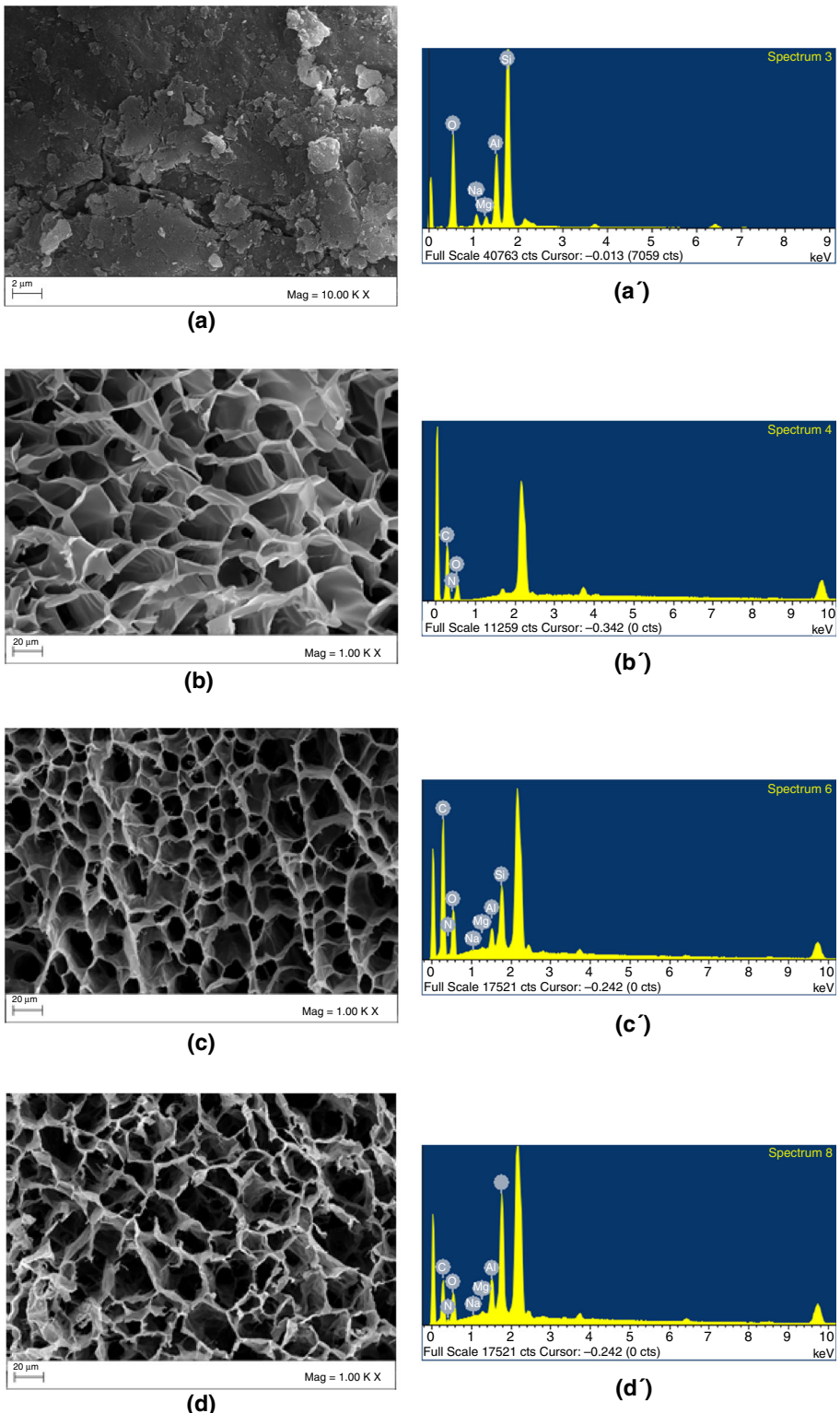

Fig. 1 SEM micrographs of: **a** Cloisite-Na^+, **b** PMAA/0-nanoclay, **c** PMAA/10-nanoclay, **d** PMAA/20-nanoclay and EDS spectra of: **a**' Cloisite-Na^+, **b**' PMAA/0-nanoclay, **c**' PMAA/10-nanoclay, **d**' PMAA/20-nanoclay. Cloisite-Na^+ micrograph was obtained at ×10,000 magnification, and the size of the bar is 2 µm. Hydrogel and all nanocomposites were obtained at ×1000 magnification, and the size of the bar is 20 µm. All SEM micrographs and EDS properties were obtained by applying an accelerating voltage of 20.0 kV using secondary electron detector

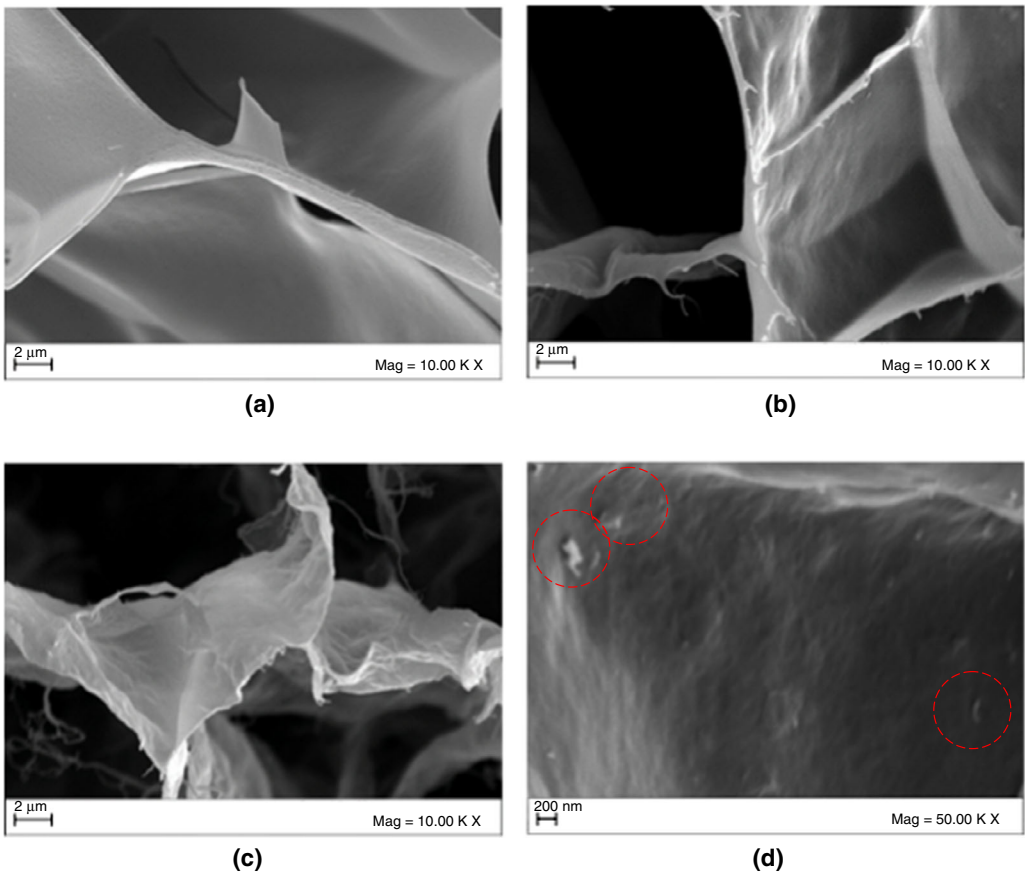

Fig. 2 SEM images of: **a** PMAA/0-nanoclay and **b** PMAA/10-nanoclay, **c** PMAA/20-nanoclay and **d** agglomeration focus of nanoclay in the walls of the hydrogel. All SEM micrographs were obtained by applying an accelerating voltage of 20.0 kV using secondary electron detector

nanoclay (Table 2). This is a good indicator of incorporation of Cloisite-Na^+ into hydrogel matrix as well as its strong interaction with the polymer, corroborating with the results presented in Fig. 2d. Probably, the metals into nanoclay structures act as a thermal catalyst, helping to evaporate the water molecules. In addition, as nanoclay is in interior or in wall of porous of the nanocomposites, there is now a competition with interaction points that before occupied by only water molecules. Thus, their presence reduced the amount of bond water (or first water) that are the water molecules interacting with hydrophilic groups of hydrogels (carboxylic and/or amide groups) and nanoclay (hydroxyl groups) [29].

Additionally, the shift in second endothermic peak to high temperature confirmed the improvement in thermal properties of the nanocomposites, corroborating with TG results. T_i of this thermal event was increased from 169 to 177 °C when the nanoclay concentration was increased from 0 to 15 mass/%, being that event is probably related to the heat released to decarboxylation of the PMAA polymer. Similar behavior was reported by Natkanski et al. [13] in the poly(acrylic acid)/montmorillonite (MMT) composites. Finally, DSC analysis did not show the glass transition of the material.

Controlled release

Figure 6 shows the KH_2PO_4 release curves of the hydrogels containing 0 and 20% of nanoclay. The release kinetic curves indicated a first sharp fertilizer release. Likely, in this stage, the nutrient release was present on the surface of the hydrogel, i.e., weakly linked. After, the nutrient release becomes slower, and this remaining sustained until the end of the study. Moreover, even after the hydrogel without nanoclay be to reach the equilibrium (around 50 h), the hydrogel containing 20% nanoclay keeps releasing, achieving the equilibrium around 75 h. In addition, the amount of nutrient released from nanocomposite was around 70% higher than hydrogel matrix. That is, this value increased from 22 to 37.5 mg g^{-1} as observed in Fig. 6b. Due to its lamellar structure, the nanoclay is contributing to increasing the interaction between fertilizer and the matrix, slowing its release.

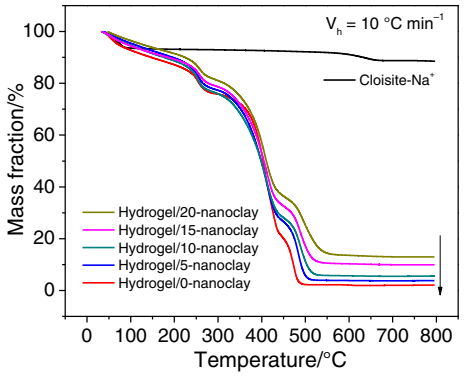

Fig. 3 TG curve of PMAA, nanoclay and of nanocomposites PMAA/n-nanoclay

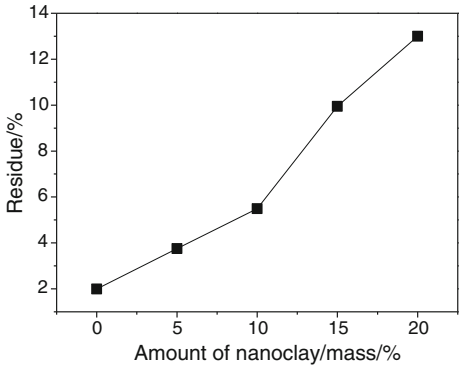

Fig. 4 Final residue in (%) of the nanocomposites obtained from thermal decomposition at 700 °C

Table 1 Initial (T_i), final (T_f) and maximum mass loss (T_{max}) temperature values of thermal events for different nanocomposites obtained from TG–DTG technique

Hydrogel/%	2^0 event				3^0 event			4^0 event		
	T_i/°C	T_{max}/°C	T_f/°C	% min °C^{-1}	T_i/°C	T_{max}/°C	T_f/°C	T_i/°C	T_{max}/°C	T_f/°C
0	198.5	253.2	293.7	0.694	302.2	406.6	445.7	445.7	474.1	510.4
5	200.6	254.6	291.6	0.678	300.1	412.3	447.8	447.8	484.1	528.8
10	201.4	254.6	285.9	0.651	290.9	412.3	451.4	451.4	488.4	543.7
15	205.6	257.5	288.1	0.514	300.1	410.9	451.4	451.4	488.4	553.7
20	203.5	256.1	288.7	0.472	304.4	408.1	454.3	454.3	494.8	577.1

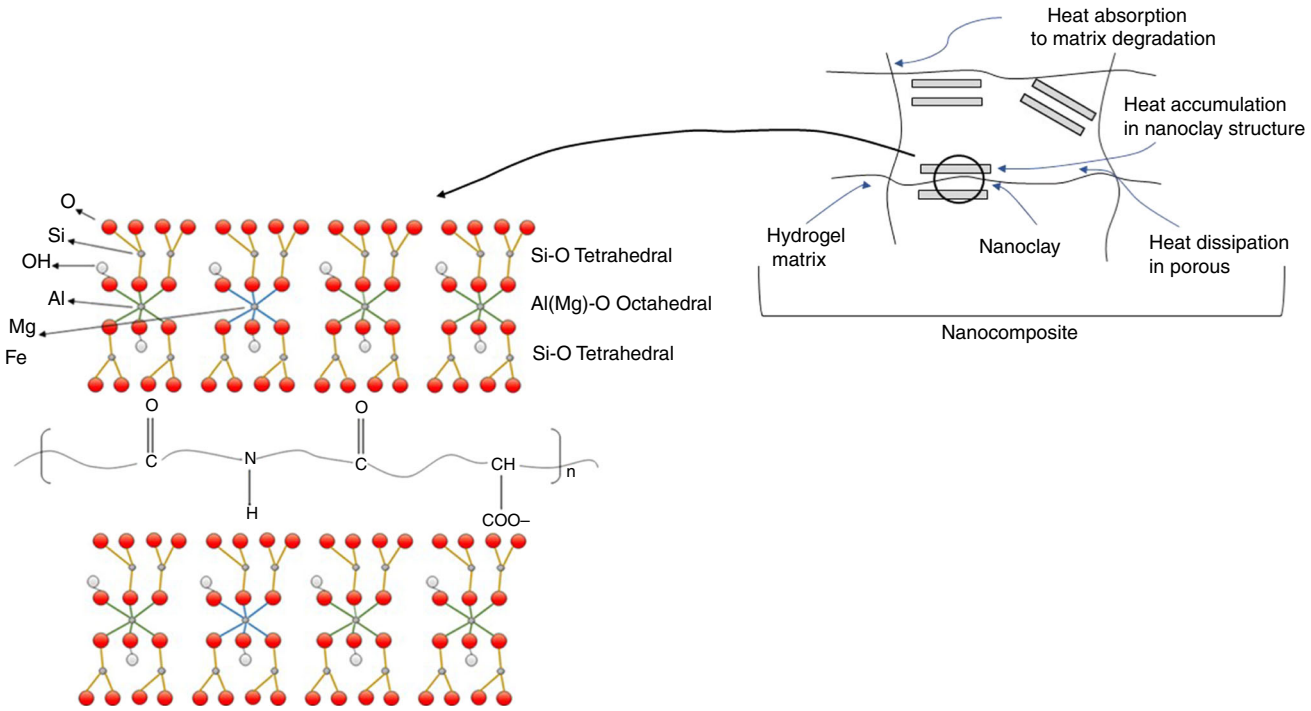

Scheme 1 Possible heat interaction–dissipation mechanism into nanocomposites

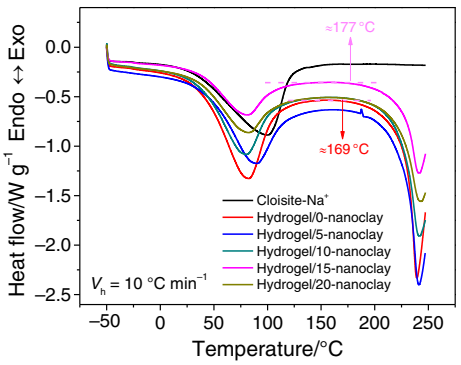

Fig. 5 DSC curves of PMAA, nanoclay and nanocomposites PMMA/n-nanoclay

Table 2 Initial (T_i) and final (T_f) temperatures and enthalpy variation (ΔH) values of different nanocomposites obtained from DSC technique

Hydrogel/%	T_i/°C	T_f/°C	ΔH/J g^{-1}
0	21.9	124.5	214.6
5	12.3	132.6	176.1
10	13.9	125.5	168.8
15	12.6	128.6	104.5
20	15.5	121.4	111.3

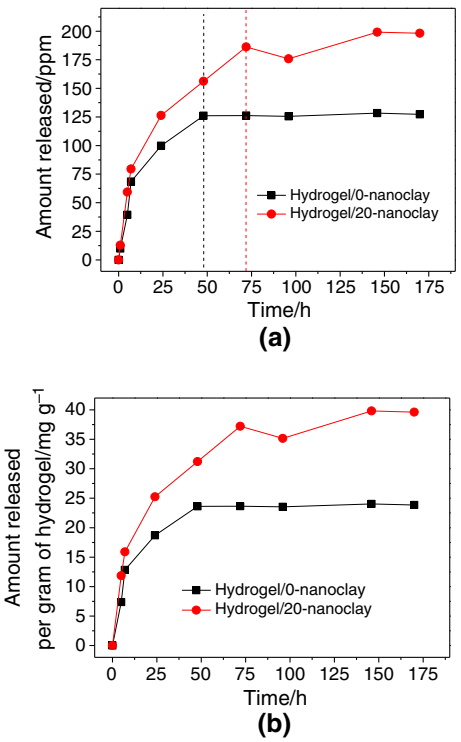

Fig. 6 **a** Profile of controlled release in ppm and **b** profile controlled release per gram of hydrogel of KH_2PO_4 for the hydrogels with 0–20% of nanoclay

Table 3 Swelling degree in the equilibrium of hydrogels with 0 and 20% of nanoclay in distilled water, after immersion in KH_2PO_4 solution and after its release in water

Hydrogel/%	Q_e in H_2O/g g^{-1}	Q_e after absorption/g g^{-1} 2000 ppm	Q_e after release/g g^{-1} 2000 ppm
0	37.87 ± 0.65	15.11	51.33
20	50.77 ± 2.13	21.90	62.12

After the sorption and desorption processes, the swelling degree of the nanocomposites was again calculated, as listed in Table 3. The saline effect has a strong influence on the swelling degree at equilibrium stage (Q_e) of the hydrogels as discussed previously in our studies [16]. Here, the reduction in Q_e after the adsorption process had the same tendency in water. In addition, there is an increase in Q_e for both materials after the release of the nutrient when compared to the Q_e values in pure water. Probably, the spaces before occupied by fertilizer molecules (higher than water molecules) are now occupied by the water molecules, increasing the water absorption.

Conclusions

SEM micrographs confirmed that the basic structure of all nanocomposites was very similar. However, it was possible to visualize the change in the surface texture of the nanocomposites in relation to the pure matrix, indicating the incorporation of the nanoclay into the polymer matrix. Furthermore, the nanocomposite containing 20% nanoclay showed the largest pores size around 15.0 ± 0.3 μm. EDS analysis confirmed the presence of the nanoclay incorporated in the polymeric matrix, and an increase in the concentrations of ions belonging of nanoclay was observed with increasing of nanoclay amount in the nanocomposite forming-solution.

By TG technique, it was possible to confirm the thermal stability of Cloisite-Na^+ pure and the increase in residue as increase in nanoclay into nanocomposites. Besides, an improvement in thermal stability of the nanocomposites caused by incorporating of nanoclay was observed, reducing around 30% of degradation rate. DSC technique showed a decrease in energy necessary to vaporize the water of hydration in the nanocomposites, indicating that the nanoclay acts as physical cross-linker. Also, an increase in initial temperature of thermal event related to decarboxylation of the PMAA polymer was observed, confirming an improvement in the thermal properties of the nanocomposites with the incorporation of nanoclay.

The controlled release investigation, even preliminary, showed a good potential of the nanocomposites for application as carrier vehicles for fertilizer controlled release systems, being that this potentiality needs to be further investigated. For instance, the capability of desorption of nanocomposites increased around 70% in relation to control matrix, reaching 37.5 mg of KH_2PO_4 released per gram of nanocomposite.

Acknowledgements The authors are grateful to Universidade Estadual Paulista, and Brazilian research financing institutions Fundação de Amparo à Pesquisa do Estado de São Paulo (FAPESP), Conselho Nacional de Desenvolvimento Científico e Tecnológico (CNPq) and Coordenação de Aperfeiçoamento de Pessoal de Nível Superior (CAPES) for their financial support.

References

1. Deng H, Song J, Elom AK, Xu J, Fan Z, Zheng C, Xing Y, Deng K. Synthesis and controlled release behavior of biodegradable polymers with pendant ibuprofen group. Int J Polym Sci. 2016;2016:5861419. doi:10.1155/2016/5861419.
2. Silva PCD, Portela AS, Lima RSC, Santana CP, Medeiros ACD, da Silva MO. Compatibility study between lipoic acid with polymers used in controlled drug release systems. J Therm Anal Calorim. 2016;123:965–71.
3. Wu L, Liu M. Preparation and properties of chitosan-coated NPK compound fertilizer with controlled-release and water-retention. Carbohydr Polym. 2008;72:240–7.
4. Pourvajadi A, Doulabi M, Soleyman R, Sharif S, Egthesadi SA. Synthesis and characterization of a novel (salep phosphate)-based hydrogel as a carrier matrix for fertilizer release. React Funct Polym. 2012;72:667–72.
5. Bortolin A, Aouada FA, Mattoso LHC, Ribeiro C. Nanocomposite PAAm/methyl cellulose/montmorillonite hydrogel: evidence of synergistic effects for the slow release of fertilizers. J Agr Food Chem. 2013;61:7431–9.
6. Pourjavadi A, Farhadpour B, Seidi F. Synthesis and investigation of swelling behavior of new agar based superabsorbent hydrogel as a candidate for agrochemical delivery. J Polym Res. 2009;16:655–65.
7. Rashidzadeh A, Olad A. Slow-released NPK fertilizer encapsulated by NaAlg-g-poly(AA-co-AAm)/MMT superabsorbent nanocomposite. Carbohydr Polym. 2014;114:269–78.
8. Raafat AI, Eid M, El-Arnaouty MB. Radiation synthesis of superabsorbent CMC based hydrogels for agriculture applications. Nucl Instrum Meth B. 2013;283:71–6.
9. Bhuyan M, Dafader NC, Hara K, Okabe H, Hidaka Y, Rahman M, Khan MMR, Rahman N. Synthesis of potato starch-acrylic-acid hydrogels by gamma radiation and their application in dye adsorption. Int J Polym Sci. 2016;2016:9867859. doi:10.1155/2016/9867859.
10. Guilherme MR, Aouada FA, Fajardo AR, Martins AF, Paulino AT, Davi MFT, Rubira AF, Muniz EC. Superabsorbent hydrogels based on polysaccharides for application in agriculture as soil conditioner and nutrient carrier: a review. Eur Polym J. 2015;72:365–85.
11. Jovanovic J, Stankovic B, Adnadjevic B. Kinetics of isothermal dehydration of equilibrium swollen PAAG hydrogel under the microwave heating conditions. J Therm Anal Calorim. 2017;127:655–62.
12. Anyszka R, Bielinski DM, Pedzich Z, Szumera M. Influence of surface-modified montmorillonites on properties of silicone rubber-based ceramizable composites. J Therm Anal Calorim. 2015;119:111–21.
13. Natkanski P, Kustrowski P, Białas A, Surman J. Effect of Fe^{3+} ions present in the structure of poly(acrylic acid)/montmorillonite composites on their thermal decomposition. J Therm Anal Calorim. 2013;113:335–42.
14. Li J, Li Y, Dong H. Controlled release of herbicide acetochlor from clay/carboxylmethylcellulose gel formulations. J Agric Food Chem. 2008;56:1336–42.
15. Wilpiszewska K, Spychaj T, Pazdzioch W. Carboxymethyl starch/montmorillonite composite microparticles: properties and controlled release of isoproturon. Carbohydr Polym. 2016;136:101–6.
16. Wang Q, Wang G, Cheng Z. Oscillatory swelling behavior of hydrogels incorporated with ion exchange nanoparticle. Drug Deliv Lett. 2011;1:58–61.
17. Junior CRF, de Moura MR, Aouada FA. Synthesis and characterization of intercalated nanocomposites based on poly(-methacrylic acid) hydrogel and nanoclay cloisite-Na^+ for possible application in agriculture. J Nanosci Nanotechnol. 2017;17:5878–83.
18. Mallakpour S, Dinari M. Preparation and characterization of new organoclays using natural amino acids and Cloisite Na^+. Appl Clay Sci. 2011;51:353–9.
19. Panic VV, Madzarevic ZP, Volkov-Husovic T, Velickovic SJ. Poly(methacrylic acid) based hydrogels as sorbents for removal of cationic dye basic yellow 28: kinetics, equilibrium study and image analysis. Chem Eng J. 2013;217:192–204.
20. Mallakpoura S, Moslemi S. Dispersion of chiral amino acid organomodified Cloisite Na^+ in poly(vinyl alcohol) matrix for designing of novel bionanocomposite films. Prog Org Coat. 2012;74:8–13.
21. Lapides I, Borisover M, Yariv S. Thermal analysis of hexadecyl trimethylammonium–montmorillonites. J Therm Anal Calorim. 2011;105:921–9.
22. Solhi L, Atai M, Nodehi A, Imani M. A novel dentin bonding system containing poly(methacrylic acid) grafted nanoclay: synthesis, characterization and properties. Dent Mater. 2012;28:1041–50.
23. Zhang Y, Jin Q, Zhao J, Wu C, Fan Q, Wu Q. Facile fabrication of pH-sensitive core–shell nanoparticles based on HEC and PMAA via template polymerization. Eur Polym J. 2010;46:1425–35.
24. Yang M. On the thermal degradation of poly(styrene sulfone)s. V. Thermogravimetric kinetic simulation of polyacrylamide pyrolysis. J Appl Polym Sci. 2002;85:1540–8.
25. Gupta B, Gautam D, Anjum S, Saxena S, Kapil A. Radiation synthesis of nanosilver nanohydrogels of poly(methacrylic acid). Radiat Phys Chem. 2013;92:54–60.
26. Mallakpour S, Dinari M. Biomodification of cloisite-Na^+ with L-methionine amino acid and preparation of poly(vinyl alcohol)/organoclay nanocomposite films. J Appl Polym Sci. 2012;124:4322–30.
27. Dumitrescu AM, Lisa G, Iordan AR, Tudorache F, Petrila I, Borhan AI, Palamaru MN, Mihailescu C, Leontie L, Munteanu C. Ni ferrite highly organized as humidity sensors. Mater Chem Phys. 2015;156:170–9.
28. Valderruten NE, Valverde JD, Zuluaga F, Ruiz-Durántez E. Synthesis and characterization of chitosan hydrogels cross-linked with dicarboxylic acids. React Funct Polym. 2014;84:21–8.
29. Pisis P, Kyritsis A. Hydration studies in polymer hydrogels. J Polym Sci Pt B Polym Phys. 2013;51:159–75.